Proceedings of ASME Turbo Expo 2011
GT2011
June 6-10, 2011, Vancouver, British Columbia, Canada

GT2011-45772

Theoretical and Experimental Investigation on Nonlinear Characterization of Metal Rubber

Hong Jie, Zhu Bin, Ma Yanhong
School of Jet Propulsion, Beihang University

Mail Address: 405 Group, Beihang University, Beijing 100191 PR. China;
Tel: +86-10-82313803; E-mail Address: hongjie@buaa.edu.cn

ABSTRACT

Metal Rubber (MR) can be widely used in many aspects such as damping of blade and support, pipe and equipment in air space technology, vehicle and ship. A theoretical method was performed to describe hysteretic properties and nonlinear stiffness and damping characteristics of Metal Rubber component. Spiral wire was considered as the micro-element structure of MR material by analyzing the manufacture process of MR component. Based on the material mechanics and coulomb friction theory, a mechanical model of spiral wire was established which is combined with the cylindrical compression coil spring theory. It was easy to explain the mechanism of hysteresis loop and the nonlinear stiffness and damping characteristic of MR component by means of analyzing contact conditions of micro-element. The quasi-static experiments were conducted to MR component with different material parameters. The influencing laws of material parameters on the performance of MR component were studied. The research was valuable for the analysis of the material mechanics and the design of MR component. It provides theoretical support for the further engineering application of MR material in the field of vibration reduction.

1 INTRODUCTION

Metal Rubber material is a kind of new-style porous damping material. The term MR arises from the similarity between the properties of metal and rubber. So it is named Metal Rubber. It formed by wires through choiceness, encircling wiredrawing, weaving and molding by compression. The special production techniques make its characteristics incomparable, such as: 1) High elasticity; 2) High damping; 3) Light weight; 4) Strong environmental adaptability; 5) Controlled porosity; 6) Easy-to-shape. Thus its applications include equipment, vibration dampers, sound absorption, filters, heat shields, and seals.

MR first named Metal mesh in 1960s which was used to settle the apparatus's vibration in the military aircraft. Child[1] in 1978 reported bench tests performed on metal mesh dampers in efforts to solve rotordynamic stability problems in the space shuttle main engine fuel turbopump. MR dampers were also used to solve subsynchronous instability problems and high synchronous vibrations for the LE-7 liquid hydrogen turbopump by Okayasu et al[2]. Zarzour and J.M.Vance[3] in 2000 studied on the characteristics of metal mesh bearing damper's stiffness and damping. AL-Khateeb[4] in 2002 studied the influence of stiffness and damping characteristics of metal mesh on loading parameters, which are the thickness of pre-compression, amplitude, frequency, lubrication, temperature and durability. While Ertas[5] in 2004 has also completed ring test for stiffness and damping at low temperature. Ring test of four kinds of metal mesh dampers were for stiffness and damping was conducted by Ertas[6] in 2008.

Metal Rubber Laboratory (MRL) in Beihang University has been researching on MR since 1993. In theory: MRL analyzed the mechanism of vibration damping[7] and the thermodynamic and sound-absorbing characteristics, and constructed the mechanical constitutive relationship of stiffness and damping characteristics[8] of MR. In design method: MRL obtained the technical parameters' selection methods according to different MR dampers with different vibration damping effect in various working conditions[7]. In techniques and equipments: MRL made mature and reliable process techniques, and developed the universal clamps, moulds and equipments to manufacture MR products. MRL has developed a series of MR products, including the ones used to reduce the vibration of rotor [10]. MRL now has founded the methods and standards to design various dampers by the use of MR material. In addition to these efforts, a series of MR dampers, including the ones used to reduce the vibration of rotor [11], were developed based on the detailed theoretical and loading experimental study on MR and combined with different engineering backgrounds. Overall, MR products have been used in many devices and have achieved observable practical engineering value.

The previous study is focused on theoretical and experimental research on the stiffness and damping model, but some important physical factors in those models and methods are not clear. Too many experiments are needed to confirm the value of these parameters and it will introduce more cost to design MR components. Due to the nonlinear characteristic of MR material, there is no method to predict the vibrating response of structure with MR component at present. Because of that the problem of developing methods in order to provide accurate, fast and robust predictive tools for the analysis of Metal Rubber under operating conditions is a problem of major practical importance.

This paper is focused on establishing a constitutive material model of MR to describe its stiffness and damping based on micro-element model. The main work is to analyze the mechanics characteristics of micro-element structure of MR and the influencing laws of material parameters on stiffness and damping.

2 CHARACTERISTICS OF HYSTERESIS CURVE

When MR component is subjected by the compression force p, the friction force F is generated by slipping which occurs between neighboring spiral wires inside MR component. Hysteretic property contains the loading force P_1, the unloading force P_2, the elastic force L and the friction force F. The cyclic hysteretic curve encircled by the loading curve and unloading curve reveals the damping property of MR material in one cycle. The difference between the loading force and unloading force represents the friction force. The middle curve represents the elastic force. During the loading process, the loading force P_1 is composed of elastic force and friction force which is given in Eq.1 as follows. It is equivalent to reduce the effect of compression force. The stiffness of MR component increases because the friction force hinders the increase of deformation. During unloading process, the unloading force P_2 is given in Eq.2 as follows. The friction force hinders the recovery deformation. Thereby, the stiffness of MR component decreases with the decrease of recovery force.

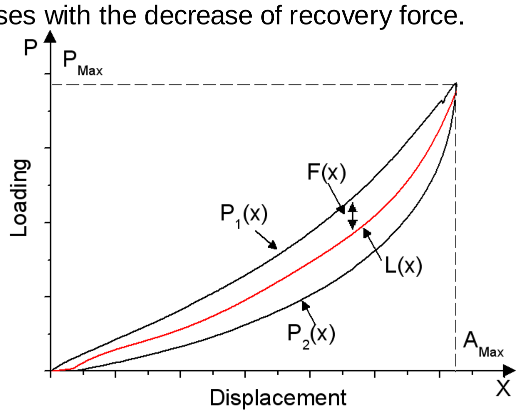

Fig.1 Hysteresis Curve of MR Component

$$P_1(x) = L(x) + F(x) \tag{1}$$

$$P_2(x) = L(x) - F(x) \tag{2}$$

Form Fig.1, the mean stiffness is given in Eq.3[10].

$$K(x) = dL(x)/dx \tag{3}$$

The loss factor is given in Eq.4[10]. Where ΔW represents energy dissipated in one cycle, it is the area encircled by hysteretic curve. U represents maximal potential energy, it is the area under the midline.

$$\eta = \frac{\Delta W}{\pi U} \tag{4}$$

According to Eq.1, Eq.2 and Eq.4, the loss factor is described as follows:

$$\eta = \frac{\int_0^A P_1(x)dx - \int_0^A P_2(x)dx}{\pi(\int_0^A P_1(x)dx + \int_0^A P_2(x)dx)/2} = \frac{\int_0^A F(x)dx}{\pi\int_0^A L(x)dx} \tag{5}$$

From the analysis of hysteresis curve in Eq.3 and Eq.5, the elastic force and friction force are the key factors. By the way of quasi-static experiments, the stiffness and damping characteristics of MR component can be obtained based on the hysteresis curve. From Fig.2, one can see that the stiffness varies with the increase of displacement. The stiffness curve can be divided three parts: when the displacement is small, the stiffness varies linearly with the increase of displacement. The soft and rigid regions appear with the increase of displacement. In actual condition, the stiffness of MR component has soft and rigid characteristics when MR component is pre-loaded and the linear region only appears in ideal condition.

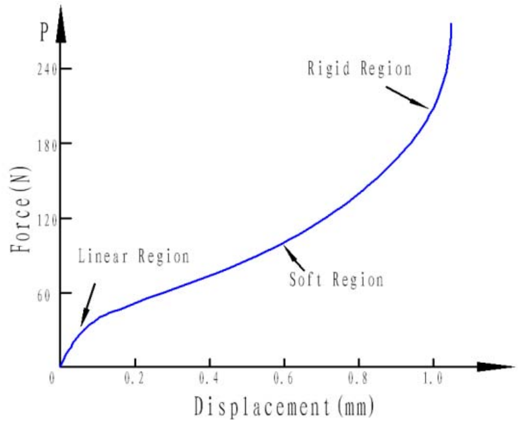

Fig.2 Stiffness Characteristics of MR Component

The effect of displacement on the damping characteristics is shown in Fig.3. The loss factor firstly increases in a small region and then it decreases with the increase of displacement with no initial displacement. In actual condition, when MR component is pre-loaded or the value of relative density is larger, the increased region does not occur.

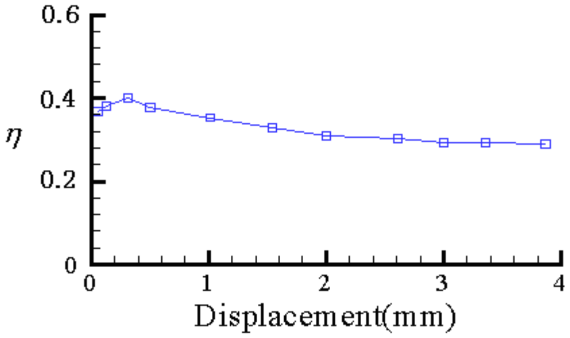

Fig.3 Damping Characteristics of MR Component

3 MICROMECHANICAL MODEL

3.1 Microstructure Model

It was easy to explain the mechanism of hysteresis loop and the nonlinear stiffness and damping characteristic by analyzed mechanics properties of microstructure model. Previous researchers studied on theoretical stiffness and damping models by using microstructure model of MR material. So far, those microstructure models of MR were too complex or not based on the structual characteristic and physical nature of MR material. Some key factors are still not clear such as the number of microstructure and the contact condition of microstructure.

According to the literature, there were four microstructure models of MR material, such as: Cantilever Beam, Pyramid, Springs and Porous Structure. Chegodayev [12] has analyzed the relationship between the helical springs by using cantilever beam and pyramid structure. It cannot be applied in engineering. Guo[13] has introduced a microelement to construct the strain-stress relation in the molding and non-molding compression direction based on the Spring Theory. It can only obtain the constitutive relation of the stiffness. Li[14] has established the nonlinear constitutive relationship on the base of the Porous Materials Theory. But the microstructure was not based on the structual characteristic of MR material.

A new constitutive material model is developed to describe the total stiffness and damping properties of MR components based on the mechanical properties of spiral wires and the relationship of neighboring spiral wires. The structure of spiral wire is shown in Fig.4 which is considered as the microelement structure of MR material by analyzing the characteristics of manufacture processing of MR component, which can describe the structual characteristic.

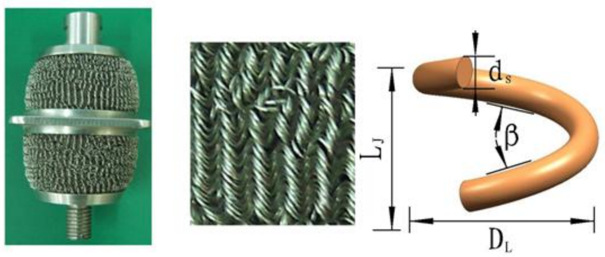

Fig.4 Microstructure of MR Materials

In order to describe the total stiffness of MR components, some parameters are necessary to be considered, such as the direction and arrangement. There are three directions: along compression modeling direction, along non-compression modeling direction, a certain angle from the compression modeling direction. There are also three arrangements: Series, Parallel and No-loading.

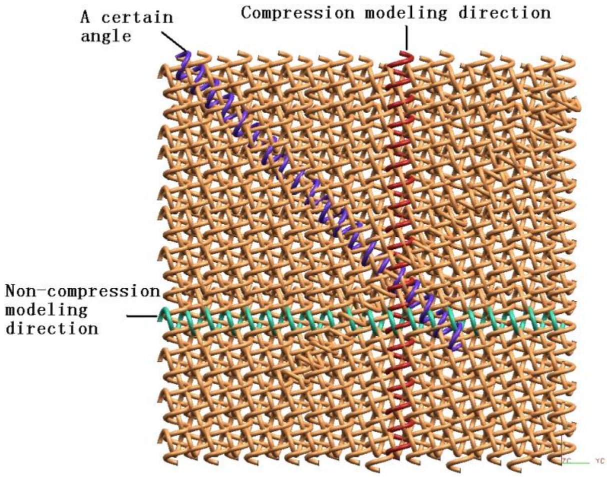

Fig.5 Directions of Spiral Wires

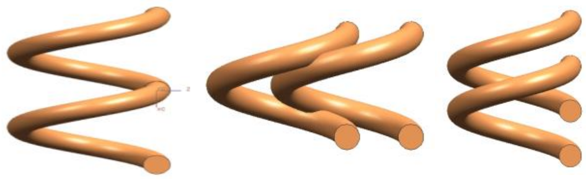

(a) Series (b) Parallel (c) No-loading

Fig.6 Arrangements of Spiral Wires

The total stiffness of MR components is the combination of spiral wire's stiffness which is caused by the interaction of series and parallel spiral wires. Stiffness curve changes from soft region to rigid region which is shown in Fig.2, that is because more spiral wires turns to be loading and the relationships between neighboring spiral wires are partially transformed from series to parallel.

Dry friction force occurred between neighboring spiral wires is the main source of MR materials' damping. There are three contact conditions: open, slipping, sticking. The slipping condition is the only source of damping.

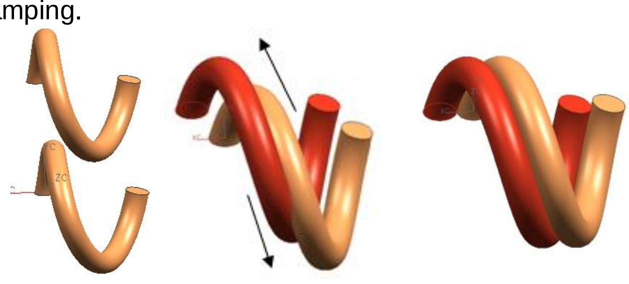

(a) Open (b) Slipping (c) Sticking

Fig.7 Contact Conditions of Spiral Wire

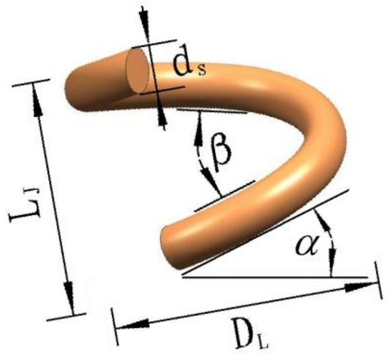

Fig.8 Microstructure Model

Therefore a spiral wire with a certain angle from the loading direction is considered as the microstructure of MR materials shown in Fig.8. The total stiffness characteristic of MR materials was described by the microstructure's stiffness and the relationship between neighboring spiral wires. The damping characteristic of MR component is described by the friction process of contact points at neighboring spiral wires.

3.2 Mechanics Properties of Microstructure

On the basis of above analysis, a spiral wire with a certain angle from the loading direction can be considered as the average of spiral wires in three directions. Three arrangements are the same in three contact conditions. So the mechanics properties of spiral wires will be obtained through the analysis on three contact conditions of microstructure model.

1) Open condition

There is gap between neighboring spiral wires, called open condition. Therefore the deformation only occurs in the upper end of spiral wire, because none of friction force and reaction force exists between them.

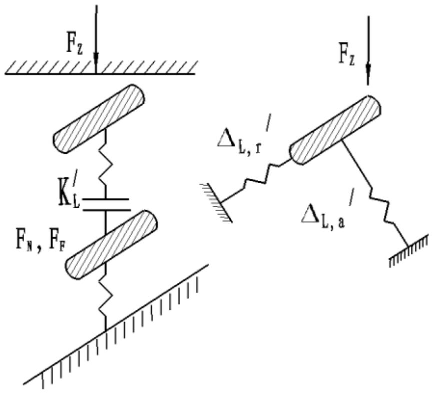

Fig.9 Micromechanical Model in Open Condition

Based on the material mechanics and cylindrical compression coil spring theory [15], when spiral wire is subjected to axis load $F_Z \cos\alpha$, the deformation of spiral wire in axial direction is defined by this equation:

$$\Delta_{L,a}{}' = \frac{F_Z \cos\alpha}{K_A} = \frac{F_Z \cos\alpha * \pi (D_L)^3 (\frac{\cos^2\beta}{GI_P} + \frac{\sin^2\beta}{EI})}{4\cos\beta} \quad (6)$$

Where, K_A is defined as follows:

$$4\cos\beta / \pi (D_L)^3 (\cos^2\beta / GI_P + \sin^2\beta / EI)$$

When spiral wire is subjected to radial load $F_Z \sin\alpha$, spiral wire is considered as a cantilever beam which is fixed at one end. The deformation of spiral wire in the radial direction is defined by this equation:

$$\Delta_{L,r}{}' = \frac{F_Z \sin\alpha}{K_R} = \frac{F_Z \sin\alpha * 8D_L^3}{Ed^4}[1+\frac{4}{3}(\frac{L_J}{D_L})^2(2+u)] \quad (7)$$

Where, K_R is defined as follows:

$$Ed^4 / 8D_L^3[1+\frac{4}{3}(\frac{L_J}{D_L})^2(2+u)]$$ [15].

According to Eq.6 and Eq.7, the deformation of spiral wires in the load direction in open condition can be obtained as follows:

$$\begin{aligned} \Delta_L{}' &= \Delta_{L,a}{}' \sin\alpha + \Delta_{L,r}{}' \cos\alpha \\ &= F_Z \sin\alpha \cos\alpha (1/K_A + 1/K_R) \end{aligned} \quad (8)$$

Therefore the stiffness of open spiral wires in the load direction can be obtained as follows:

$$K_L{}' = K_A K_R / (\sin\alpha \cos\alpha (K_A + K_R)) \quad (9)$$

During the unloading process, there is also none of friction force and reaction force, hence the stiffness of spiral wire is equal to $K_L{}' = K_U{}'$ in the unloading process,

2) Slipping condition

With the increase of load, the gap between neighboring spiral wire decreases. Parts of spiral wires which are not in contact begin to contact. At this time reaction force F_N and friction force F_f come into existence which is shown in Fig.10. With further increase of load, the tangential force at contact points also increases. When the tangential force exceeds the critical value, contact points begin to slip. At this time the lower end of spiral wire can contribute to the stiffness, which is one of the reasons that the stiffness of MR nonlinearly varies. According to the analysis of hysteresis loop, one can see that there is different in the effects of the loading process on friction force. This is the main reason for the damping of MR materials generated.

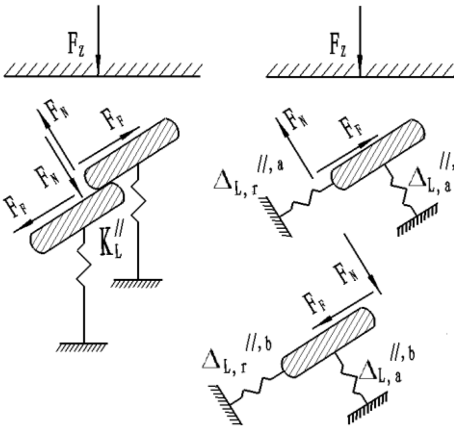

Fig.10 Micromechanical Model in Slipping Condition

The motion and deformation is different between slipping spiral wires and opening spiral wires. The wire in the upper end of spiral wires slips along the cylindrical surface of one's lower end. During the loading process, the loading force is composed of the elastic force and friction force. Therefore the spiral wire is subjected to the axis force $F_Z \cos\alpha$ and reaction force F_N. The deformation of upper slipping spiral wires in the axial direction can be defined by the following equation:

$$\Delta_{L,a}{}^{//,a} = \frac{F_Z \cos\alpha - F_N}{K_A} \tag{10}$$

At the same time, the upper end of spiral wire is subjected to radial load $F_Z \sin\alpha$ and friction force F_f, so the deformation of upper slipping spiral wire in the radial direction is defined by this equation:

$$\Delta_{L,r}{}^{//,a} = \frac{F_Z \sin\alpha - F_f}{K_R} \tag{11}$$

During loading process, the lower end of spiral wire is subjected to axis load reaction force F_N; the deformation of lower slipping spiral wire in axial direction is defined by this equation:

$$\Delta_{L,a}{}^{//,b} = \frac{F_N}{K_R} \tag{12}$$

Two spiral wires is supposed to be in slipping condition, the deformation of upper spiral wire relative to the lower one arises from slipping only in the radial direction. Thus the deformation of spiral wires in axial direction are the same, $\Delta_{L,a}{}^{//,a} = \Delta_{L,a}{}^{//,b}$.

According to Eq.10 and Eq.12, the reaction force and friction force can be obtained as follows:

$$F_N = \frac{1}{2} F_Z \cos\alpha \tag{13}$$

$$F_f = \mu F_N = \frac{1}{2}\mu F_Z \cos\alpha \tag{14}$$

According to Eq.8, Eq.10, Eq.11, Eq.13 and Eq.14, the deformation of slipping spiral wires in the load direction can be obtained as follows:

$$\begin{aligned}\Delta_L{}^{//} &= F_Z(\sin\alpha\cos\alpha / 2K_A \\ &\quad + (2\sin\alpha - u\cos\alpha)\cos\alpha / 2K_R)\end{aligned} \tag{15}$$

Therefore the stiffness of slipping spiral wires in the load direction can be obtained as follows:

$$\begin{aligned}K_L{}^{//} &= 2K_A K_R / (\sin\alpha\cos\alpha K_R \\ &\quad + (2\sin\alpha - u\cos\alpha)\cos\alpha K_A)\end{aligned} \tag{16}$$

During the unloading process, the friction force prevents the recovery deformation. Thereby, it is equivalent to reduce the effect of recovery force, the stiffness of MR decreases. The friction force changes its direction. According to the above mentioned analysis, the stiffness of slipping spiral wires in the load direction can be obtained as follows:

$$\begin{aligned}K_U{}^{//} &= 2K_A K_R / (\sin\alpha\cos\alpha K_R \\ &\quad + (2\sin\alpha + u\cos\alpha)\cos\alpha K_A)\end{aligned} \tag{17}$$

3) Sticking condition

The space decreases when the deformation increases with the increase of load. If the space disappears which is shown in Fig.11, the contact condition of spiral wires will transit from slipping into sticking. The transition of contact conditions is another reason that the stiffness of MR nonlinearly varies.

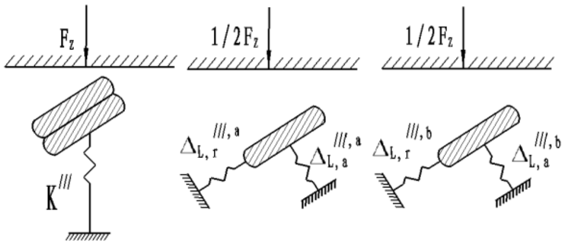

Fig.11 Micromechanical Model in Sticking Condition

Sticking spiral wire is regarded as the parallel structure. There is no relative deformation with each other. Thus every spiral wire is subjected to the half of load, $1/2F_Z$. According to Eq.8 and Eq.9, the stiffness of spiral wires is defined by this equation:

$$K_L{}^{///} = 2K_A K_R / (\sin\alpha\cos\alpha(K_A + K_R)) \tag{18}$$

During unloading process, there is also no relative deformation. Hence the stiffness of spiral wires is equal in unloading process,

$$K_L''' = K_U'''.$$

4 STIFNESS AND DAMPING MODEL OF MR

The mechanical characteristic of microelement is different when the contact conditions are different. Various kinds of contact conditions occur inside the MR components simultaneously. The transition between different contact conditions will affect the stiffness and damping characteristics of MR components.

There is a complex relationship between the spiral wires inside MR component. A certain rule can be analyzed from the results which are obtained by applied some predigestions and assumptions. After molded, MR material can be assumed to be a homogeneous material. The mechanical characteristic of micro-element is the same as the one of MR components.

MR component is assumed to consist of many layers along the molded direction. There are N_A microelements in the plane of each layer and N_L microelements in the height of each layer. The number of microelements is the same for different layers. The relationship between the microelements in the same layer is series, and the relationship between layers is parallel.

When MR component is loaded, the total equivalent stiffness can be expressed as follows:

$$K_L(x) = \frac{N_A}{N_L} k_L^e(x) = \frac{N_A}{N_L}(k_L' n_1(x) + k_L'' n_2(x) + k_L''' n_3(x)) \quad (19)$$

When MR component is unloaded, the total equivalent stiffness can be expressed as follows:

$$K_U(x) = \frac{N_A}{N_L} k_U^e(x) = \frac{N_A}{N_L}(k_U' n_1(x) + k_U'' n_2(x) + k_U''' n_3(x)) \quad (20)$$

According to Eq.5, Eq.19 and Eq.20, the loss factor can be obtained as follows:

$$\eta = \frac{\Delta W}{\pi U} = \frac{2(\int\int K_L(x)dx^2 - \int\int K_U(x)dx^2)}{\pi(\int\int K_L(x)dx^2 + \int\int K_U(x)dx^2)}$$
$$= \frac{2(k_L'' - k_U'')\int\int n_2(x)dx^2}{\pi(\int\int (2k_L' n_1(x) + (k_L'' + k_U'')n_2(x) + 2k_L''' n_3(x))dx^2} \quad (21)$$

Where n1(x), n2(x), n3(x) is the contribution ratio of the three conditions (open, slipping, sticking) to the total equivalent stiffness. From Eq.19, Eq.20 and Eq.21, one can see that the change of the ratio is the main factor which affects the stiffness and damping properties of MR component. The ratio is also influenced by the initial parameters of MR materials such as material parameters and process parameters.

After the material is defined, the total number of micro-element N_{Max} can by obtained from the follow equation [13].

$$N_{Max} = \frac{L_S \cos\beta}{\pi D_l} = \frac{4\rho_{MR} V_{MR} \cos\beta}{\rho_S \pi^2 d_s^2 D_l} \quad (22)$$

When MR component is not loaded, the open spiral wires and contacting spiral wires exit inside MR component. The ratio is affected by the relative density when the component is not loaded. The ratio of the open microelements is lager when the relative density is small. The ratio of the contact microelements is lager when the relative density is large. The relationship between them is shown in Fig. 12.

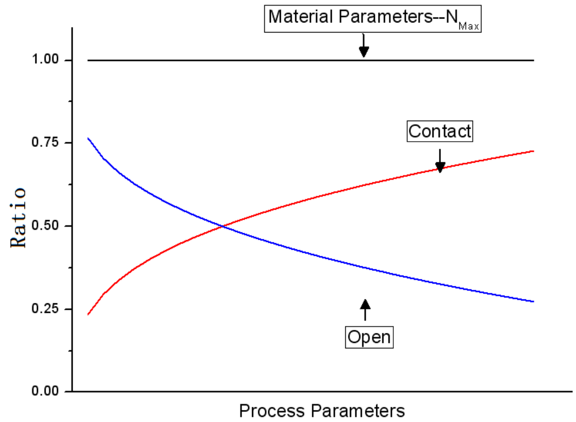

Fig.12 Effects of Process Parameters on the Initial Ratio of Contact Pairs

When MR component is loaded, the number of the open micro-elements decreases with the increase of the force level. Parts of the micro-elements begin to contact. Some contact pairs in the interface of micro-elements begin to slip and others begin to stick. At the same time, with the increase of the force level, the gap between neighboring spiral wires decreases. The contact condition of contact pair is changed from slipping to sticking. During the load process, the ratio has been changed. The curve is shown in Fig.13.

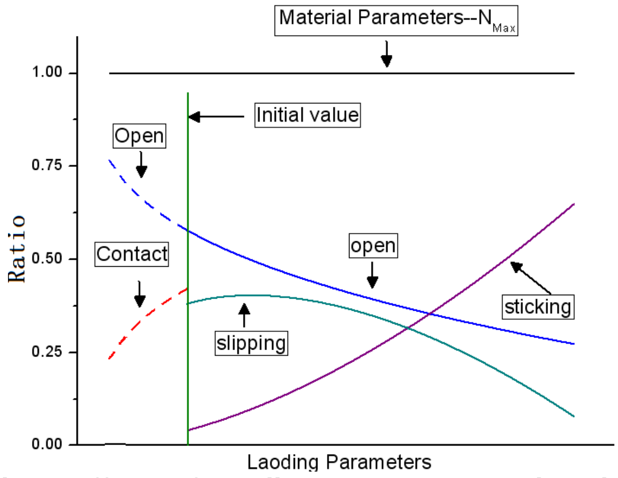

Fig 13 Effects of Loading Parameters on the Initial Ratio of Contact Pairs

From Fig.13, one can see that the mechanical characteristic and ratio of micro-element can be obtained after the material parameter and process parameter is defined. Then the total equivalent stiffness and loss factor can be calculated based on the equations and the rule of the ratio.

Three contact conditions of spiral wires have different ratio on initial condition. Three contact conditions of spiral wires were transformed ceaselessly under the dynamic loads. Ratio of slipping spiral wires and the rule of transformation are the key point of value of damping under the dynamic loads.

5 QUASI-STATIC EXPERIMENTAL RESULTS AND DISCUSSIONS

The quasi-static experiments of MR components' mechanical properties were performed using WDW3100 electronic universal testing equipment as shown in Fig. 14(a). The loading velocity is controllable, and the loads are even without impact. The velocity of the loading is about 0.25~0.5mm/s. The rate of unloading force is about 50~100N/s. they are different control mode by the WDW3100 electronic universal testing equipment. The loads were measured by the force transducer of 30KN or 1KN, while the strains were recorded by electronic micrometer.

The relative density $\bar{\rho}$, wire's diameter d_S, spiral wire's diameter D_L and D_L / d_S are the essential material parameters which influence its stiffness and damping characteristics. Considering the rule of effect, it is necessary to experiment with the four factors respectively, while the structural parameters of MR material samples are shown in Tab. 1. The diameter of MR samples is 15mm, and the thickness is 30mm. Then the result and analysis of the experiments are presented as follows.

(a) Electronic equipment

(b) MR Samples

Fig.14 Quasi-Static Experimental Test System

Tab.1 Structural Parameters of MR samples

Test ID	Relative density/%	Wire's diameter /mm	Spiral wire's diameter /mm
1	0.1	0.12	1.2
2	0.2	0.12	1.2
3	0.25	0.12	1.2
4	0.2	0.15	1.2
5	0.2	0.18	1.2
6	0.2	0.12	1.5
7	0.2	0.12	1.8
8	0.2	0.15	1.5
9	0.2	0.18	1.8

5.1 Effects of Relative Density

Taking the samples 1, 2 and 3 with different relative density for measuring, it is accessible to gain the test results about the stiffness and loss factor as shown in Fig. 15. From Fig.15 (a), one can see that stiffness increases with the increase of deformation. When the deformation is smaller than 2mm, the stiffness is almost identical corresponding to the relative density of 0.25 and 0.20. When the deformation is larger than 2.5mm, the stiffness with the relative density of 0.25 is larger than 0.2. On the other hand, the stiffness with relative density of 0.25 and 0.20 are both larger than 0.1. The loss factor decreases firstly and then tends to remain steady with the increase of deformation as shown in Fig.15 (b). Furthermore, the loss factor with relative density of 0.1 is larger than 0.20 and 0.25.

The contact condition transits from open into slipping with the increase of relative density firstly. According to the analysis of mechanic properties of microstructure, one can see that the slipping stiffness is larger than the open one and the slipping spiral wires is the main resource of damping. Thus the stiffness and damping increase. However when the relative density is larger than a certain value, the number of slipping spiral wires reaches the maximum. At the same time part of slipping spiral wires transit into sticking ones, the stiffness increases rapidly and the damping decreases. However, when the spiral wires are compressed to a certain extent, the elasticity of spiral wire turns to be weak and the ability of dissipating energy also turns to be weak. As a result, the loss factor decreases to be a certain value and remains steady.

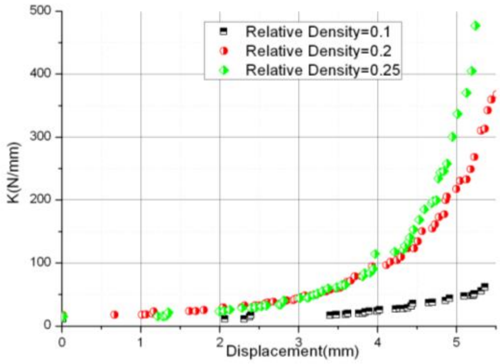

(a)

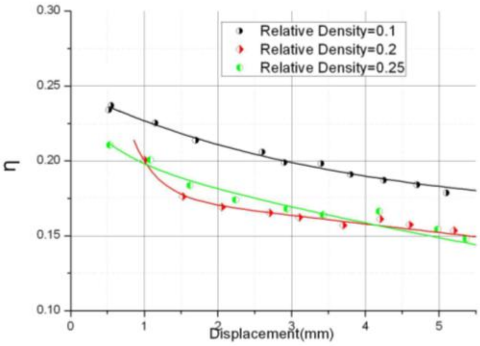

(b)

Fig.15 Effects of Relative Density on Stiffness and Loss Factor

5.2 Effects of Wire's Diameter

Taking the samples 2, 4 and 5 or 6 and 8 or 7 and 9 with different wire's diameter for measuring, the test results are shown in Fig.16. From Fig.16, one can see that with the increase of wire's diameter, the stiffness increases and the loss factor decreases. According to Eq.9, 16 and 18, the stiffness of microstructure in three contact conditions increases with the increase of wire's diameter. That is why the stiffness of MR component increases. According to Eq. 21 and 22, the total number of microelements decreases with the increase of wire's diameter. But at the same time the gap between neighboring spiral wires decreases in the same volume which equals to $D_L - d_S$, there will be more slipping spiral wires in the initial stage with the same relative density. With the increase of the number of contacting points, the contribution ratio of the slipping and sticking conditions increases, non-linear in the stiffness curve may appears in small displacement. On the other hand, the friction force increases, and so does the ability of dissipating energy.

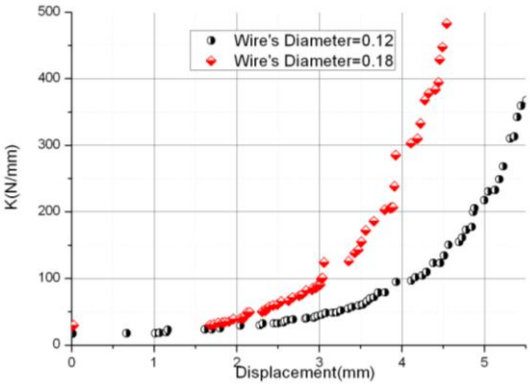

(a)

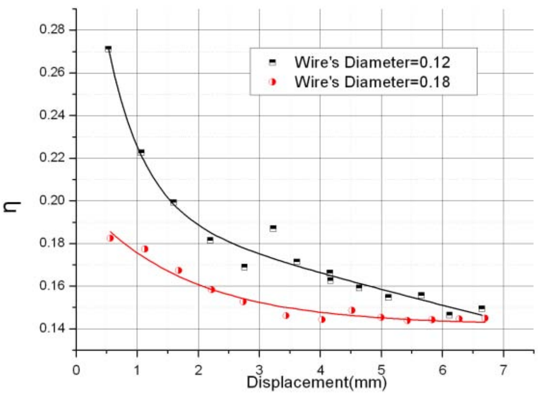

(b)

Fig.16 Effects of Wire's diameter on Stiffness and Loss Factor

5.3 Effects of Spiral Wire's Diameter

Taking the samples 2, 6 and 7 or 4 and 8 or 5 and 9 with different spiral wire's diameter for measuring, the test results are shown in Fig.17. From Fig.17, one can see that with the increase of spiral wire's diameter the stiffness decreases and the loss factor increases. The stiffness of microstructure in three conditions decreases, that means the effect is different from the one of wire's diameter. Although the total number of microelement increases, the gap between neighboring spiral wires decreases even more because of the decrease of the distance which equals to $D_L - d_S$. The number of contacting points increases. Thus the loss factor increases.

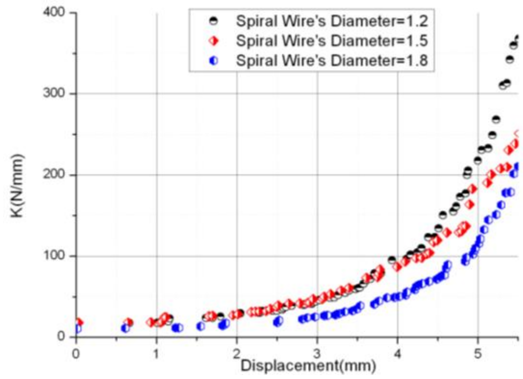

(a)

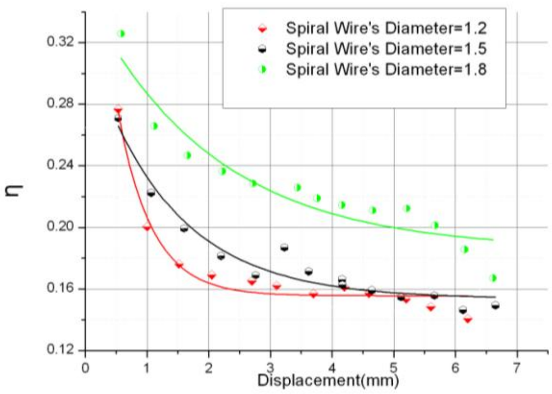

(b)

Fig.17 Effects of Spiral Wire's diameter on Stiffness and Loss Factor

5.4 Effects of Dl/ds

Taking the samples 2, 8 and 9 with different wire's diameter when Dl/ds is the same for measuring, the test results are shown in Fig.18. From Fig.18, one can see that when wire's diameter is 0.12mm, the stiffness and loss factor reach the maximum values. The reason is that the stiffness of microstructure increases and more spiral wires contribute to the stiffness of MR component. Although the total number of microelement increases with the decrease of wire's diameter and spiral wire's diameter, more contact points begin to exit in MR component.

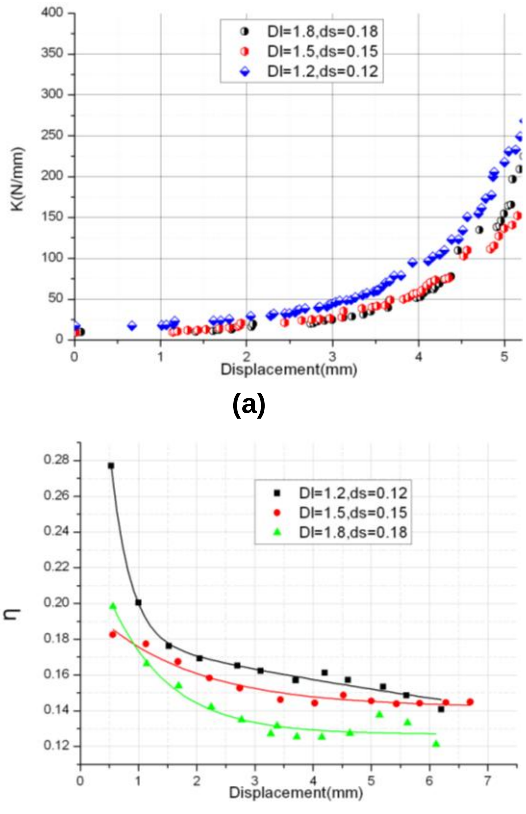

(a)

(b)

Fig.18 Effects of Dl/ds on Stiffness and Loss Factor

6 CONCLUSION

This paper is focused on the stiffness and damping characteristics of MR material form the mechanics properties of microstructure in different directions, arrangements and contact conditions and its change process under loading. The formula of stiffness and loss factor was derived. Evaluating the stiffness and damping was accomplished from the mechanics properties of microstructure and the ratio of slipping spiral wires. It was experimentally shown that variation law of the stiffness and loss factor with the relative density, wire's diameter, spiral wire's diameter and Dl/ds. The theoretical model can explain this variation law form structual characteristic and physical nature of MR.

7 NOMENCLATURE

$P_1(x)$	Loading force
$P_2(x)$	Unloading force
$L(x)$	Elastic force
$F(x)$	Friction force
X	Displacement
W	Energy dissipating in a working circle
U	Represent the maximal potential energy
η	Loss factor
d_S	Wire's diameter
D_L	Spiral wire's diameter
L_J	Helical pitch
α	Angle between the load direction and axis direction of spiral wire
β	Spiral wire's rise angle
$K_L^{/}$	Stiffness of open spiral wire during the loading process
$K_U^{/}$	Stiffness of open spiral wire during the unloading process
$\Delta_{L,a}^{/}$	Deformation of open spiral wire in axial direction
K_A	Stiffness of spiral wire in axial direction
I	Moment of inertia for spiral wire
I_P	Polar moment of inertia for spiral wire
E	Elastic modulus of wire
G	Shear modulus of wire
$\Delta_{L,r}^{/}$	Deformation of open spiral wire in radial direction
K_R	Stiffness of spiral wire in radial direction
u	Poisson ratio
$\Delta_L^{/}$	Deformation of open spiral wire in load direction
F_N	Reaction force in slipping condition
F_f	Friction force in slipping condition
$\Delta_{L,a}^{//,a}$	Deformation of upper spiral wire in the axial direction
$\Delta_{L,r}^{//,a}$	Deformation of upper spiral wire in the radial direction
$\Delta_{L,a}^{//,b}$	Deformation of lower spiral wire in the axial direction
$\Delta_L^{//}$	Deformation of slipping spiral wire in the load direction
$K_L^{//}$	Stiffness of slipping spiral wire during the loading process
$K_U^{//}$	Stiffness of slipping spiral wire during the unloading process
$K_L^{///}$	Stiffness of sticking spiral wire during the loading process
$K_U^{///}$	Stiffness of sticking spiral wire during the unloading process
$k_L^{e}(x)$	Total equivalent stiffness during the loading process
$k_U^{e}(x)$	Total equivalent stiffness during the unloading process
n	Number of micro-elements
$n_1(x)$	Ratio of contact pairs in open condition
$n_2(x)$	Ratio of contact pairs in slipping condition
$n_3(x)$	Ratio of contact pairs in sticking condition

L_S Total length of spiral wire

ρ_{MR} Density of MR component

ρ_S Density of material

V_{MR} Volume of MR component

$\bar{\rho}$ Relative density, $\bar{\rho} = \rho_{MR} / \rho_S$

REFERENCES

[1]Childs, D.W. The Space Shuttle Main Engine High-Pressure Fuel Turbopump Rotordynamic Instability Problem[J]. ASME Journal of Engineering for Power. 1978, 100: 48-57

[2]Okayasu, A., Ohta, T., Azuma, T., Fujita, T., and Aoki, H., 1990, "Vibration Problems in the LE-7 Liquid Hydrogen Turbopump," Proceedings of the 26th AIAA/SAE/ASME/ASEE 26th Joint Propulsion Conference, pp. 1–5.

[3]Zarzour, Mark, and Vance, J.M. Experimental Evaluation of a Metal Mesh Bearing Damper[J]. ASME Journal of Engineering for Gas Turbines and Power. 2000, 122(2): 326-329

[4]Al-Khateeb, E. M., 2002, "Design, Modeling, and Experimental Investigation of Wire Mesh Vibration Dampers," Ph.D. thesis, Texas A&M University, College Station, TX.

[5]Ertas, B., Al-Khateeb, E. M., and Vance, J. M., 2004, "Rotordynamic BearingDampers for Cryogenic Rocket Engine Turbopumps," J. Propul. Power, 20,pp. 674–682.

[6]Bugra H. Ertas，Huageng Luo. Nonlinear Dynamic Characterization of Oil-Free Wire Mesh Dampers, 2008, ASME, VOL.138 032503-1-8

[7]Deng Jianbo, Zhu Zigen, Li Qihan, 1997, "Theoretical and experimental investigation on characteristics of a new structure damping material-metal rubber", Ph.D. thesis, Dept of Propulsion, Beijing University of Aeronautics and Astronautics.

[8]Ma Yanhong, Hong Jie, Li Haoyu, Li Yifeng, "Theoretical analysis on sound absorption characteristics of metal rubber"[J],Journal of Beijing University of Aero. and Astro., 2009, Vol35:653-656.

[9]Ma Yanhong, Hong Jie, 2005, Theoretical and experimental investigation of a new-style adaptive squeeze flim damper, Ph.D. thesis, Dept of Propulsion, Beijing University of Aeronautics and Astronautics.

[10]Ma Yanhong, Wang Hong, Li Haoyu, Hong Jie. Study on Metal Rubber Material's Characteristics of Damping and Sound Absorption. Proceedings of ASME TURBO EXPO 2008, Berlin, Germany, GT2008-50961

[11]Ma Yanhong, Hong Jie, Zhang Dayi, Wang Hong. Study of Transient Characteristic of a Simple Rigid Rotor Supported on a Squeeze Film Damper with Valvular Metal Rubber Squeeze Film Ring. Proceedings of ASME TURBO EXPO 2007, Montreal, Canada, GT2007-27585

[12] Chegodayev D E (Russia) etc , Ed. by L I Zhong2e etc. The Designing of Components Made of Metal Rubber .Beijing: Industry Publishing Company of National Defence , 2000

[13]Chen Yanqiu , Guo Baoting , Zhu Zigen , The Inestigation of the Stiffness Characteristics and the Stress-Strain Relation of Metal Rubber .Journal of Aerospace Power,2002,17 (4) :416～420

[14]Li Yuyan, Investigation on Nonlinear Constitutive Relationship and Vibration Response of System for Elastic Porous Metallic Rubber, Xian Jiaotong University, Xian Ph.D. Thesis.2005

[15]Zhang Yinghui, Luo Shengguo etc, Spring. Beijing: China Machine Press,1980

